Cell Biol Toxicol (2025) 41:34
https://doi.org/10.1007/s10565-025-09989-3

RESEARCH

Manganese exposure induces parkinsonism-like symptoms by Serpina3n-TFEB-v/p-ATPase signaling mediated lysosomal dysfunction

Huihui Hong · Sicheng Liu · Ting Yang · Jinxian Lin · Kun Luo · Yudong Xu · Ting Li · Yu Xi · Lingling Yang · Yuan-Qiang Lu · Wei Yuan · Zhou Zhou

Received: 11 June 2024 / Accepted: 3 January 2025

Abstract Manganese (Mn) is a neurotoxin that has been etiologically linked to the development of neurodegenerative diseases in the case of overexposure. It is widely accepted that overexposure to Mn leads to manganism, which has clinical symptoms similar to Parkinson's disease (PD), and is referred to as parkinsonism. Astrocytes have been reported to scavenge and degrade extracellular α-synuclein (α-Syn) in the brain. However, the mechanisms of Mn-induced neurotoxicity associated with PD remain unclear. Serpina3n is highly expressed in astrocytes and has been implicated in several neuropathologies. The role Serpina3n plays in Mn neurotoxicity and PD pathogenesis is still unknown. Here, we used wild-type and *Serpina3n* knockout (KO) C57BL/6 J mice with i.p. injection of 32.5 mg/kg $MnCl_2$ once a day for 6 weeks to elucidate the role of Serpina3n in Mn-caused neurotoxicity regarding parkinsonism pathogenesis. We performed behavioral tests (open field, suspension and pole-climbing tests) to observe Mn-induced motor changes, immunohistochemistry to detect Mn-induced midbrain changes, and Western blot to detect Mn-induced changes of protein expression. It was found that *Serpina3n* KO markedly alleviated Mn neurotoxicity in mice by attenuating midbrain

Supplementary Information The online version contains supplementary material available at https://doi.org/10.1007/s10565-025-09989-3.

H. Hong · S. Liu · J. Lin · K. Luo · Z. Zhou (✉)
Department of Environmental Medicine, School of Medicine, Chongqing University, Chongqing, China
e-mail: lunazhou00@cqu.edu.cn

T. Yang · W. Yuan (✉)
Department of Otolaryngology, Chongqing General Hospital, Chongqing University, Chongqing, China
e-mail: weiyuan175@sina.com

Y. Xu
Department of Environmental Medicine, Zhejiang University School of Medicine, Hangzhou, China

T. Li · Y.-Q. Lu (✉)
Department of Emergency Medicine, School of Medicine, The First Affiliated Hospital, Zhejiang University, Hangzhou, China
e-mail: luyuanqiang@zju.edu.cn

T. Li · Y.-Q. Lu
Zhejiang Provincial Key Laboratory for Diagnosis and Treatment of Aging and Physic-Chemical Injury Diseases, Hangzhou, China

Y. Xi
Beijing Advanced Innovation Center for Food Nutrition and Human Health, Beijing Technology and Business University, 100048 Beijing, China

L. Yang
Department of Occupational Health, Third Military Medical University, 400038 Chongqing, China

Published online: 23 January 2025

dopaminergic neuron damage and ameliorating motor deficits. Furthermore, using immunofluorescence colocalization analysis, Western blot and quantitative real-time PCR on Mn-treated C8-D1A cells, we found that *Serpina3n* KO significantly improved astrocytic α-Syn clearance by suppressing Mn-induced lysosomal dysfunction. Reduced transcription factor EB (TFEB)-v/p-ATPase signaling is responsible for the impairment of the lysosomal acidic environment. These novel findings highlight Serpina3n as a detrimental factor in Mn neurotoxicity associated with parkinsonism, capture the novel role of Serpina3n in regulating lysosomal function, and provide a potential target for antagonizing Mn neurotoxicity and curing parkinsonism in humans.

Keywords Manganese · Neurotoxicity · Parkinsonism · Serpina3n · Lysosomal dysfunction

Abbreviations

α-Syn	α-Synuclein
ATP6V1A	ATPase H + Transporting V1 Subunit A
ATP6V1B2	ATPase, H + transporting, lysosomal VI subunit B, isoform 2
ATP6V1C1	V-type ATPase protein subunit C1
ATP6V1D	ATPase H + Transporting V1 Subunit D
ATP6V1E1	ATPase H + Transporting V1 Subunit E1
ATP6V1H	H subunit of V-ATPase
ATP6V1G1	ATPase H + Transporting V1 Subunit G1
ATP6V13A2	ATPase H + Transporting V0 Subunit A2
CTSB	Cathepsin B
CTSD	Cathepsin D
Gabarap	GABA Type A Receptor-Associated Protein
Gba	Glucocerebrosidase
GFAP	Glial Fibrillary Acidic Protein
GNS	Glucosamine (N-Acetyl)-6-Sulfatase
Gusb	Beta-glucuronidase
Lamp1	Lysosome-associated membrane protein 1
Lamp2	Lysosome-associated membrane protein 2
Mn	Manganese
Pak1	P21-regulated kinase 1
PD	Parkinson's disease
P-ATPases	P-type ATPases
Rac1	Ras-related C3 botulinum toxin substrate 1
Sgsh	N-Sulfoglucosamine Sulfohydrolase
Snca	Synuclein Alpha
SNpc	Substantia nigra compacta
TFEB	Transcription Factor EB
TPP1	Tripeptidyl Peptidase 1
Uvrag	UV Radiation Resistance Associated
V-ATPases	Vacuolar-type, proton-translocating ATPases

Introduction

Manganese (Mn), a vital trace element, is important for human health and is involved in many physiological processes. Mn is widely distributed in the environment and is used in various industrial fields such as steel smelting, dry cell manufacturing, etc. Combustion of gasoline containing MMT also releases Mn compounds into the air. In recent years, Mn contamination of air, soil and water has become a matter of great public concern worldwide (O'Neal and Zheng 2015; Vollet et al. 2016). For instance, the average airborne Mn concentration at a ferro-Mn alloy plant during the rainy season was 3 times higher than the US EPA criteria (0.05 μg/m^3) (Menezes-Filho et al. 2009). In addition, Mn concentration in well water in North Carolina have reached 4 mg/L (> 2 times above the health limit), posing a serious threat to those who rely on private well water for their livelihood (Gillispie et al. 2016). Occupational cases of manganism have already been reported in many countries (Jiang et al. 2006; Lucchini et al. 2018). It has been assumed that Mn-associated neurotoxicity is similar to, but not identical with, parkinsonism (Calne et al. 1994). However, a large number of studies have consistently reported a correlation between exposure to Mn in both environmental and occupational settings and the development of neurodegenerative diseases with Parkinson-like symptoms, which manifest as motor deficits and cognitive impairment (Andruska and Racette 2015; Karri et al. 2016).

Parkinson's disease (PD) refers to the neurodegenerative disease that is traditionally been identified by specific motor deficits, substantial nigral neuronal loss and the pathological presence of α-Syn

aggregates in neurons (Ye et al. 2023). Typically, immunoreactive cytoplasmic inclusions of α-Syn in neurons appear to be a hallmark of parkinsonism (Mor et al. 2019). The recognition of the central role of α-Syn in PD has been of great importance in understanding the degenerative process that occurs in this disease. Recently, it has become widely accepted that exposure to environmental risk factors is critical in the etiology of human PD (Harischandra et al. 2019; Ma et al. 2020; Morello et al. 2008). In addition, excessive Mn uptake is preferentially deposited in astrocytes and promotes α-Syn aggregation in the midbrain. Generally, astrocytes rarely generate α-Syn but scavenge misfolded α-Syn released from surrounding neurons to maintain brain homeostasis (Booth et al. 2017; Lee et al. 2008). Extracellular pathological α-Syn could be rapidly taken up by astrocytes for subsequent degradation (Lindstrom et al. 2017). A previous study suggested that the TLR-4 mediated inflammatory response of astrocytes may ultimately exacerbate α-Syn accumulation (Fellner et al. 2013; Rannikko et al. 2015). While the endogenous lysosomal degradation machinery is a central pathway for the degradation of α-Syn aggregates (Jiang et al. 2024). Numerous studies have shown that lysosomal dysfunction is linked with α-Syn pathogenicity and contributes to the initiation and progression of PD (Wang et al. 2020). Notably, excessive Mn exposure has been suggested to cause astrocytic defects in lysosomal function and cytotoxicity (Fan et al. 2010). Zhang et al. found that Mn reduced nuclear localization of TFEB and disrupted autophagic-lysosomal degradation of mitochondria in mouse striatum astrocytes (Zhang et al. 2020a). However, it remains unclear whether lysosomal dysfunction is involved in Mn-induced astrocytic toxicity and inability to clear α-Syn.

Serpina3n is a secretory serine protease inhibitor that is highly abundant in brain astrocytes and participates in various physiological functions and pathologies (Aslam and Yuan 2020). Elevated levels of Serpina3n were detected in the cerebrospinal fluid and brains tissues of individuals suffering from neurodegenerative conditions (Porcellini et al. 2008). As reported, there may be a potential link between Serpina3n upregulation and amyloid beta peptide aggregation in Alzheimer's disease, based on single-nucleus transcriptomics of the mouse brain (Zhou et al. 2020). In parallel, Serpina3n-mediated axonal injury and neuronal death through inhibition of granzyme B activity has also been documented in animal models (Haile et al. 2015). Increased expression of Serpina3n in the dorsal root ganglia has also been found after nerve injury, which attenuates neuropathic pain by inhibiting leukocyte elastase (Vicuna et al. 2015). In our recent research, we uncovered that Serpina3n has a pivotal role in trimethyltin-caused neurotoxic astrocytic activation and memory deficits in mice (Xi et al. 2019). Therefore, we speculated that Serpina3n may be a specific functional target for environmental chemical-induced neurotoxicity. Serpina3n may also exert a vital influence on Mn neurotoxicity, and engage in pathogenesis of Mn-induced parkinsonism-like symptoms.

To this end, we first investigated the effects of *Serpina3n* knockout (KO) on Mn-induced pathological changes and neurobehaviour in mice. To determine the astrocytic clearance capacity of α-Syn, C8-D1A cells were used as an *in vitro* model for the determination of neurotoxicity and lysosomal impairment. Lysosomal acidic environment, cathepsin B (CTSB) and cathepsin D (CTSD) activity, expression of v/p-ATPases were measured. The *Serpina3n* KO C8-D1A cell line was also established to verify the role of Serpina3n in regulating TFEB-mediated lysosomal function and α-Syn degradation in relation to Mn-induced parkinsonism-like symptoms. Our results demonstrate that *Serpina3n* KO attenuated Mn-induced α-Syn accumulation by preserving lysosomal function in astrocytes. Mn exposure leads to Serpina3n-mediated lysosomal dysfunction in astrocytes attributed to TFEB-v/p-ATPases signaling, thereby inducing α-Syn accumulation. Taken together, this study provides new mechanistic insights into Mn-induced parkinsonism-like symptoms, identifies Serpina3n as a potent detrimental factor for lysosomal function, and highlights the possibility of targeting Serpina3n to antagonize Mn neurotoxicity concerning parkinsonism.

Materials and methods

Generation of Serpina3n KO mice and animal treatments

Serpina3n KO (Serpina3n$^{-/-}$) mice were produced by using CRISPR/Cas9 system to delete Serpina3n

exon 2–5 (Gempharmatech. Co., Ltd, China) (Zhang et al. 2020b). sgRNA/Cas9 expression plasmid was designed and constructed. A selection of four sgRNAs, each with optimal cleavage efficacy, were used to target the specified regions. These sgRNA transcripts were then precisely microinjected along with Cas9 mRNA into individual fertilized eggs of the C57BL/6 J strain, resulting in the generation of the baseline F0 mouse. These F0 mice were then mated with C57BL/6 J mice to generate the subsequent F1 generation. DNA sequencing and PCR were employed to evaluate the genotype of mice. The genotyping primers were shown in Table S1. The PCR amplification outcomes differentiated between the WT allele (454 bp), and the KO allele (~ ~ 700 bp).

Eight-week old C57BL/6 J mice, both wild-type (WT) and genetically modified Serpina3n$^{-/-}$ (KO) mice, were maintained under standardized conditions with a 12-h light/dark cycle and unrestricted access to food and water. Following a one-week acclimatization, the animals were systematically allocated into four groups (14 mice each, with a sex ratio of 1 female to 1 male): the WT-control group (WT-Con), the KO-control group (KO-Con), the WT-Mn group (WT-Mn) and the KO-Mn group (KO-Mn). Mice in WT-Mn and KO-Mn groups received intraperitoneal injection of 32.5 mg/kg $MnCl_2$ (Sigma-Aldrich, 203,734, USA) dissolved in saline once a day for 6 weeks (8 a.m. to 9 a.m.). The dose of Mn exposure was chosen based on previous studies and our preliminary results (data not shown) (Deng et al. 2015; Qi et al. 2020b). Mice in WT-Control and KO-Control groups mice were intraperitoneally injected with the same volume of saline solution. After 6 weeks, neurobehavioral tests were conducted in all mice of different groups. Upon completion of the study, the mice were humanely euthanized through CO_2 asphyxiation, adhering to ethical guidelines. The midbrain tissues of the mice were promptly separated and stored at − 80 °C for subsequent study. The entire animal study was conducted under the approval of the Zhejiang University Ethnics Committee of Animal Care and Research, with the approval number RN 2019–771-1. All procedures followed the National Institutes of Health's Guide for the Care and Use of Laboratory Animals.

Neurobehavioural tests

The neurobehavioral tests employed in the study were conducted as previously reported (Chen et al. 2015). Open field test was performed a day after the final injection. Suspension test and pole-climbing test were carried out the next day after open field test to estimate motor function. The averaged values of score and time were then utilized for statistical analyses. All mice were allowed to acclimatize environment for 30 min in advance.

Open field test was performed to measure exploratory activity (Kim et al. 2019; Masini and Kiehn 2022; Ommati et al. 2020). In the experimental setup, each mouse was gently placed in the center of the box. The box is white plastic and measures 45 cm × 45 cm × 45 cm. A video camera was used to monitor the movement of each animal for 10 min (Any-maze, Stoelting, USA). Immobile time, locomotory speed, traveled distance and center time were recorded.

The suspension test was employed to evaluate the coordination of the mouse's limb movements, mice were suspended by their forepaws from a horizontal wire in an open box, and their performance was observed (30 s). Mice performance was rated based on a scheme, ranging from 0–5 (Tong et al. 2022). 0: subject mice fell off the wire. 1: subject mice two forepaws grasped the wire. 2: in addition to 1, subject mice tried to use their hind paws to climb onto the wire. 3: Two front paws and one or two back paws of the subject mice were suspended from the wire. 4: subject mice hung from the wire with all four paws, tail wrapping around wire. 5: subject mice escaped.

The pole-climbing test was also used to determine the motor coordination ability of mice (Ma et al. 2016). Mice were placed on a soft rubber plug, which is on the top of a wooden pole. The pole was 50 cm high and had a diameter of 0.5 cm. Time (s) for mice climbing down without interference was measured.

TH immunohistochemistry analysis

Mice were sacrificed and perfused with 0.9% saline. The brains were then removed and fixed in 4% paraformaldehyde. Following fixation, the brains were dehydrated through a series of increasing concentrations of sucrose solution (20% and 30%) for 48 h, respectively. Dehydrated brains were then embedded

in paraffin. Substantia nigra compacta (SNpc) and striatum sections were defined based on anatomical landmarks and all TH-stained sections were obtained from the same anatomical region of the SNpc. The brain paraffin blocks were cut into Sects. (5 μm). Tissue slices were subjected to treatment with the TH primary antibody (Abcam, ab112, UK) and incubated at 4 °C overnight in a wet box. Brain slides were washed using PBS, and secondary antibody was added. After one-hour incubation in room temperature avoiding light, the light microscope (Zeiss, LSM 880, Germany) was used for image acquisition. Areas of the midbrain from 4 mice (sex ratio 1 female to 1 male) were assigned for semi-quantification analysis using Image J. As previously described, IHC Profiler plugin was used to calculate the average optical density (AOD) and percentage of TH positive neurons (Crowe and Yue 2019).

Cell culture and treatment

C8-D1A cells belong to a mouse astrocytic type I cell line clone expressing GFAP. The C8-D1A cell line was purchased from Procell Company (Wuhan, China). CRISPR/Cas9 system was employed to generate *Serpina3n* KO C8-D1A astrocyte cell line by deleting Serpina3n exon 2–5 (Cyagen Biosciences Inc., Guangzhou, China) as previously described (Leonard et al. 2017). A selection of four sgRNAs, each with optimal cleavage efficacy, were used to target the specified regions. Successful establishment of *Serpina3n* KO cell line was confirmed by the mRNA level determination of Serpina3n in cells.

WT and *Serpina3n* KO cells were cultured in DMEM (Gibco, USA) supplemented with 10% FBS (PAN, Germany), penicillin and streptomycin (Gibco, USA). Cells were cultured in an environment with 5% CO_2 humidification and maintained at 37 °C. $MnCl_2$ (Sigma-Aldrich, 203,734, USA) were diluted with distilled deionized water. 0.8 μg/mL mouse α-Syn protein (Abcam, ab246002, UK) was used to determine the astrocytic α-Syn clearance capacity (Lee et al. 2008).

Cell viability analysis

To assess cell viability, we used CCK-8 kit (DONJINDO, CK04, Japan). Firstly, C8-D1A cells were seeded and cultured in 96-well plates. After described treatments, the original medium was replaced with the fresh medium mixed with 10% CCK-8 reagents. Plates were incubated at 37 °C for 1 h. OD value at the absorbance of 450 nm was determined via the microplate reader (Thermo, Varioskan LUX, USA).

Total RNA extraction and quantitative real-time PCR analysis

To quantify the expression of target genes, WT, *Serpina3n* KO C8-D1A cells and brain tissues following the described treatment were mixed with RNAiso Plus (TaKaRa, 9109, Japan). The spectrophotometer (Thermo Scientific, NanoDrop 2000, USA) was employed to assess RNA concentration. Extracted RNA (1 μg) was transcribed into cDNA using the corresponding kit (TaKaRa, RR820A, Japan). The expression of the targeted cDNA was quantified using the real-time qPCR instrument (Roche, LightCycler™ 480 II, Switzerland). We have listed the used primers in Table. S2. The specificity of qPCR was verified through melting curves for each trial. The statistical analysis was calculated using the Eq. $2^{-\Delta\Delta Cp}$.

Western blot

The cells or tissue samples were lysed in RIPA solution (Beyotime, P0013B, China) with cOmplete Protease Inhibitor (Roche, 4,693,132,001, Switzerland) and PhosSTOP Phosphatase Inhibitor Cocktail (Roche, 4,906,837,001, Switzerland). After protein quantification using a BCA kit (Beyotime, P0011, China), 25 μg of protein was subjected to electrophoretic separation by SDS-PAGE (12–20%). After transferring to PVDF membranes (0.2 μm), membrane blocking was conducted in 5% nonfat powdered milk for 2 h. The blocked membranes were then incubated with antibodies against α-Syn (BD Bioscience, 610,787, USA), Serpina3n (R&D, AF4709, USA), LAMP1 (Invitrogen, PA1-654, USA), LAMP2 (Invitrogen, PA1-655, USA) and GAPDH (Proteintech, 10,494–1-AP, USA) overnight at 4 °C. After 3 washes with TBST, membranes were incubated with corresponding second antibodies for 1 h. Protein bands were visualized after the last 3 washes with TBST. Targeted protein expression was evaluated by ImageJ software (NIH, USA).

Immunofluorescence analysis

In immunofluorescence analysis for brain tissues, mice were sacrificed and perfused with 0.9% saline. The brains were then removed and fixed in 4% paraformaldehyde. Following fixation, the brains were dehydrated through the sucrose solution (30%) at 4 °C overnight. Frozen block of the brains was sliced into Sects. (20 μm) utilizing Cryostat (Thermo, CryoStar NX50, USA). Tissue slices were treated with 0.5% TritonX-100/PBS solution for 10 min and then incubated with antibodies targeting Serpina3n (R&D, AF4709, USA), GAFP (Abcam, ab7260 or ab279290, UK), α-Syn (Abcam, ab1903, UK) or LAMP1(Abcam, ab24170, UK) overnight, respectively. After washing with 0.5% TritonX-100/PBS, tissue sections were incubated with corresponding secondary antibodies for 2 h. Alexa FluorTM Plus 488 or 567 (Invitrogen, A32814, A21202, A10037, A21206 and A10042, USA) conjugated with fluorophores. DAPI working solution was employed for visualizing nuclei. A research slide scanner (OLYMPUS, VS200, Japan) was used for image acquisition.

In immunofluorescence analysis for cells, WT and Serpina3n KO cells seeded on coverslips were treated as described and fixed with immunofixative solution. After blockage using sheep serum (working solution) (ZSGB-BIO, ZLI-9056, China), primary antibodies targeting TFEB (Protein tech, 13,372–1-AP, China), GAFP (Abcam, ab7260 or ab279290, UK) and α-Syn (Abcam, ab1903, UK) were added in slides, respectively, and incubated at 4 °C overnight away from light. After 3 washes with PBS, slides were incubated with second antibody (Beyotime, A0453, China) for 1 h. DAPI working Solution was used for nucleus visualization. Zeiss confocal laser scanning microscope was used for images capturing (Zeiss, LSM880, Germany). For immunofluorescence quantification, 8 non-overlapping areas of the midbrain of 4 mice (sex ratio 1:1) were assigned colocalization coefficients. Coloc 2 analysis was conducted to calculate colocalization coefficient using Fiji based on Pearson's correlation coefficient (Dunn et al. 2011).

Determination of lysosomal functions

The LysoSensor Green DND-189 dye was used to detect lysosomal pH (Invitrogen, L7535, USA). C8-D1A cells plated on a 96-well plate were loaded with 1 μmol/L LysoSensor Green DND-189 at a condition of 37 °C for 5 min. A multi-function microplate reader (Biotek, SynergyMx M5, USA) was employed to read the fluorescence intensity at excitation/emission wave of 485/530 nm.

The catalytic activities of CTSB and CTSD were measured to indicate lysosomal function by using CTSB (BioVision, K140-100, USA) and CTSD (BioVision, K143-100, USA) activity assay kits based on previously described method (Li et al. 2016).

Statistical analysis

Statistical analyses were performed by either *t*-test for two-groups comparison or one-way ANOVA followed by Tukey's post hoc analysis for four-group comparison using GraphPad Prism (GraphPad Software, 8.0.1, USA). Semi-quantification of optical density (OD) for immunohistochemistry was performed using ImageJ software (NIH, USA). The co-localisation analysis for immunofluorescence was conducted using Fiji software (NIH, USA) with the plugin Coloc 2, based on Pearson's correlation coefficient. Differences were considered significant at $P < 0.05$.

Results

Serpina3n KO mitigated Mn induced parkinsonism-like symptoms in mice

Serpina3n plays a critical role in astrocyte-mediated neuroinflammation (Xi et al. 2019). Since neuroinflammation is generally accepted as the key pathological event in parkinsonism, we hypothesized that Serpina3n might exert a detrimental effect in Mn neurotoxicity in relation to parkinsonism. To verify our hypothesis, we first deleted *Serpina3n* gene in C57BL/6 J mice using the CRISPR/cas9 technique to generate *Serpina3n* KO mice (Fig. S1A). WT and *Serpina3n* KO mice were treated with intraperitoneal injection of 32.5 mg/kg $MnCl_2$ (once a day) for 6 weeks to determine changes in the locomotor activities of the mice. *Serpina3n* KO did not induce any detectable effect on the health and the body weight in mice during the experiment (Fig. S1B). The Open field test indicated that mice in WT-Mn group showed a decreased total distance traveled, decreased speed of movement, a shorten residence time in the center

area, as well as increased time spent immobile compared to the WT-Con group (Fig. 1A-E; all $P < 0.001$ vs WT-Con). The pole-climbing and the suspension tests showed an elevation in trial time and a reduction in trial scores, respectively, compared to the WT-Con group, (Fig. 1F-G; all $P < 0.001$ vs WT-Con).

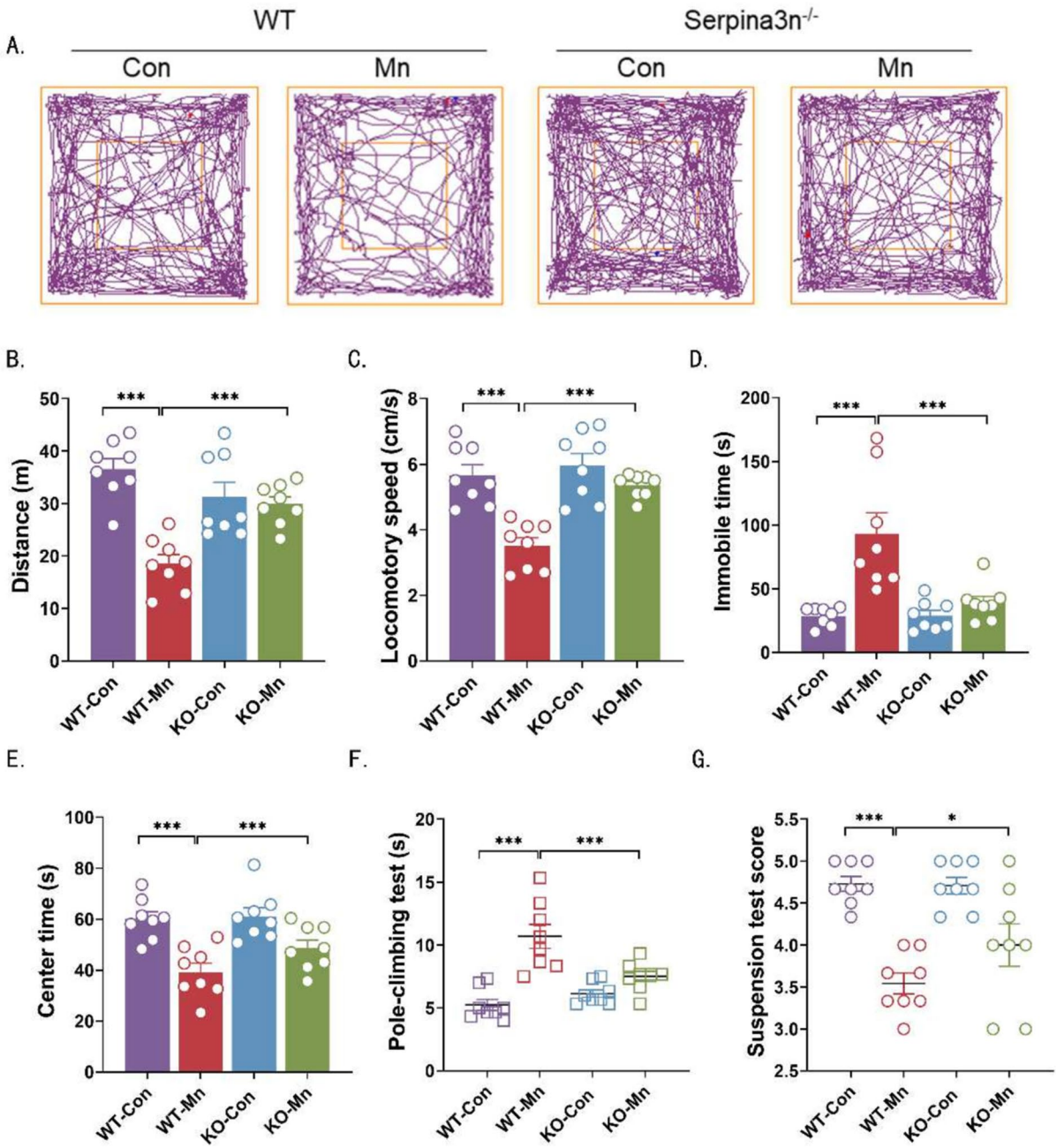

Fig. 1 *Serpina3n* KO mitigated Mn induced parkinsonism-like symptoms in mice. Wild type and *Serpina3n* KO mice were treated with $MnCl_2$ (32.5 mg/kg, i.p.) once a day for 6 weeks. A-E: Open field test. (**A**) diagram showing mice movement in the central or peripheral regions, (**B**) distance traveled (m), (**C**) locomotory speed (cm/s), (**D**) immobile time (s). (**E**) center time (s). **F**: Pole-climbing test. **G**: Suspension test. n = 8. The values are presented as means ± SEM. $^{*}p < 0.05$, $^{**}p < 0.01$, $^{***}p < 0.001$

As speculated, *Serpina3n* KO significantly ameliorated Mn-induced locomotor abnormalities (Fig. 1A-E, G; $P < 0.001$; Fig. 1F, $P < 0.05$). Thus, Serpina3n deletion mitigated Mn induced parkinsonism-like symptoms.

Serpina3n KO ameliorated Mn-induced α-Syn accumulation in mice midbrain

Parkinsonism is a neurodegenerative condition recognized by distinctive motor deficits and substantia nigral neuronal loss (Moors et al. 2016). As shown in Fig. 2A and Fig. S2A, Mn resulted in marked dopaminergic neuronal loss, characterized by fewer TH^+ neurons, in the SNpc and striatum, which was attenuated by Serpina3n deletion in mice (Fig. 2B-C and Fig. S2B). Clinicopathological and neuroimaging studies strongly indicated that α-Syn generated from neurons contribute to initial motor manifestations of parkinsonism and the preceding neuronal loss (Ma et al. 2020; Mor et al. 2019). Hence, we investigated the consequence of Serpina3n deletion on Mn-induced α-Syn accumulation. First of all, Mn markedly elevated the protein level of Serpina3n in mice midbrain. (Fig. 2D-E). Meanwhile, *Serpina3n* KO induced an obvious decrease in α-Syn protein level in the midbrain in KO-Mn group in comparison to WT-Mn group (Fig. 2F, $P < 0.05$). Interestingly, the mRNA level of Snca gene encoding α-Syn was not changed after Mn exposure (Fig. 2G), suggesting that Mn does not affect α-Syn biosynthesis but interferes with α-Syn clearance, leading to α-Syn accumulation in the midbrain. It is widely acknowledged that astrocytes play a critical role in the clearance of α-Syn (Booth et al. 2017). More importantly, our previous study demonstrated that Serpina3n is primarily located in astrocytes (Xi et al. 2019). To investigate a possible functional relationship between Serpina3n and astrocytic α-Syn clearance, we performed immunofluorescence co-localization analysis of α-Syn and GFAP proteins in astrocytes. α-Syn was found in GFAP-labelled astrocytes, indicating that astrocytes take up extracellular α-Syn. Serpina3n deletion significantly mitigated Mn-induced increase in α-Syn immunofluorescence in striatal astrocytes (Fig. 2H-I), suggesting a protective clearance of α-Syn in astrocytes. Taken together, our data show that deletion of Serpina3n ameliorated Mn-induced α-Syn accumulation in the mouse midbrain.

Mn induced cytotoxicity and disrupted Serpina3n-mediated α-Syn clearance in C8-D1A cells

As the most abundant glial cells in the brain, astrocytes are indispensable mediators of α-Syn toxicity because of their capacity to internalize α-Syn released from dysfunctional neurons. In parallel, astrocytic activation and dysfunction are also important contributors to the development of parkinsonism. Thus, C8-D1A cells were treated with indicated concentrations of $MnCl_2$ for a period of 24 h to verify the detrimental impacts of Mn on astrocytes *in vitro*. The result showed that Mn at 50 μmol/L induced a significant reduction in cell viability in C8-D1A cells ($P < 0.01$ compared to Con group; Fig. 3A). Meanwhile, the mRNA levels of astrocytic activation marker *Gfap* was increased ($P < 0.05$ compared to Con group in 50 μmol/L; Fig. 3B). Meanwhile, Mn induced a dose-dependent downregulation of the mRNA expression of *Pak1* and *Rac1*, which are negative regulators of astrocyte activation (Fig. 3C-D). As anticipated, Mn resulted in a dose-dependent elevation in the protein level of Serpina3n (Fig. 3E-F). Therefore, we established a *Serpina3n* KO C8D-1A cell line to determine whether Serpina3n is involved in the process of astrocytic α-Syn clearance. We used CRISPR to KO Serpina3n in the C8-D1A cells, and the efficacy of the KO was confirmed by the qPCR analysis compared with the WT C8-D1A cells treated with Mn (Fig. 3G). Next, mouse α-Syn protein (0.8 μg/mL) was added to the cultures to determine the clearance ability of α-Syn in C8D-1A cells with or without Mn treatment (50 μmol/L) for 24 h. Our preliminary data showed that 0.8 μg/mL alpha-synuclein had no toxic effects on C8-D1A cells (data not shown). It was suggested that Mn treatment significantly promoted α-Syn accumulation and suppressed α-Syn clearance in astrocytes, whereas *Serpina3n* KO reversed these effects (Fig. 3H-I). Our data showed that Mn induced cytotoxicity and disrupted Serpina3n-mediated α-Syn clearance in C8-D1A cells.

Mn impaired lysosome function in C8-D1A cells

Lysosomal dysfunction is increasingly recognized as a central event in the pathophysiology of PD, as lysosomal dysfunction may contribute to α-Syn aggregation (Moors et al. 2016). Recent reports suggest that

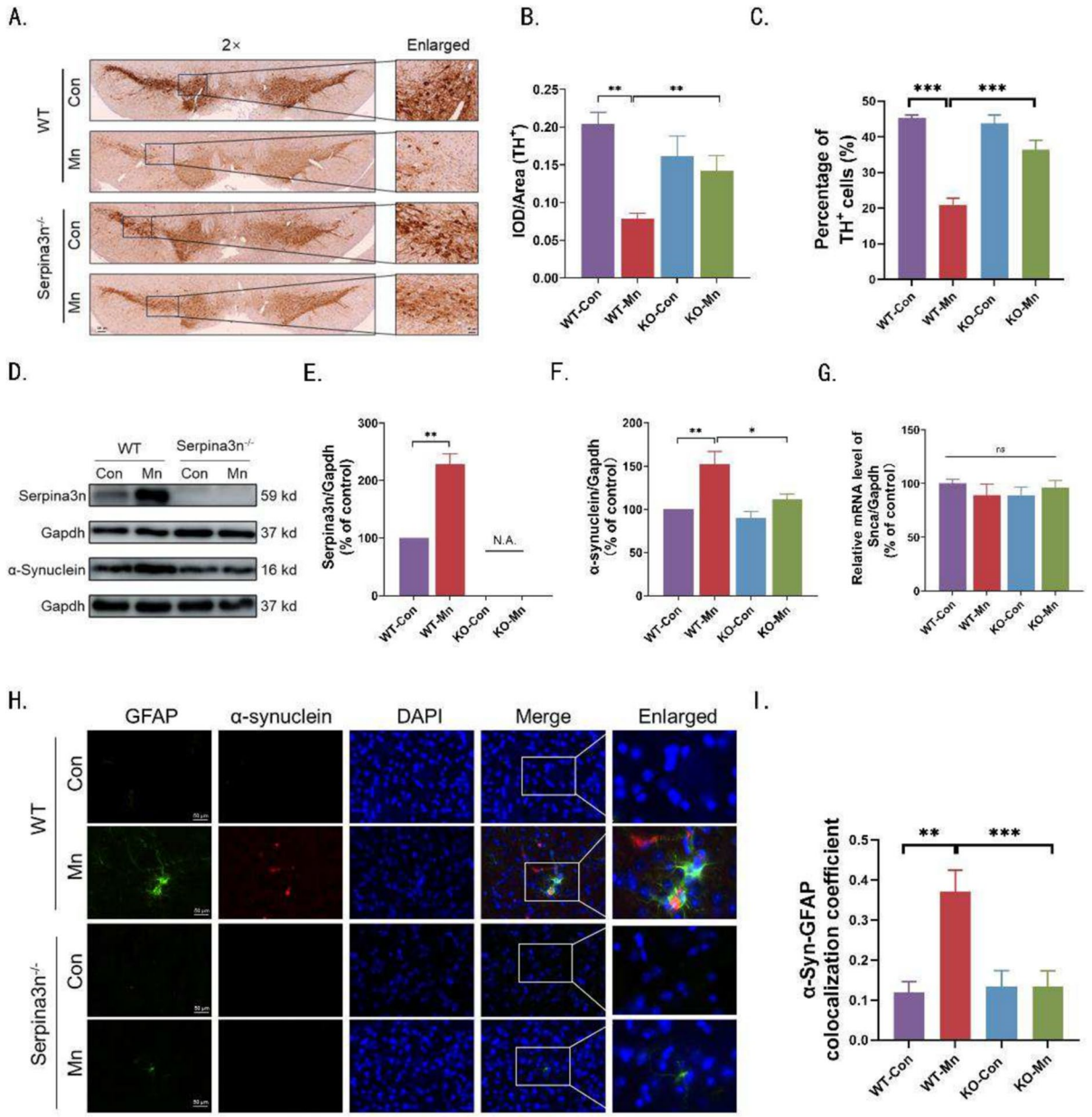

Fig. 2 *Serpina3n* KO ameliorated Mn-induced α-Syn accumulation in the mouse midbrain. **A**: Histopathological changes indicated by tyrosine hydroxylase staining in mouse midbrain. **B**-**C**: Semi-quantitative analysis of TH positive neurons ($n=4$). **D**-**F**: The protein level of α-Syn and Serpina3n in mice midbrain and their semi-quantification ($n=6$). **G**: The mRNA level of *Snca* in mice midbrain ($n=6$). **H**: Immunofluorescent co-localization of GFAP with α-Syn and semi-quantification analysis in mice striatum. Scale bar: 50 μm. **I**: 8 non-overlapping areas of the midbrain of 4 mice (sex ratio 1:1) were assigned for semi-quantitative analysis. The values are presented as means ± SEM. N.A. means not available. * $p<0.05$, ** $p<0.01$

lysosomal PH defects occur in a growing number of neurodegenerative diseases (Colacurcio and Nixon 2016). To verify whether lysosomal dysfunction is involved in Mn-induced astrocytic toxicity, Lysosensor™ Green DND-189 reagents were used to indicate changes in lysosomal H^+ concentration after Mn

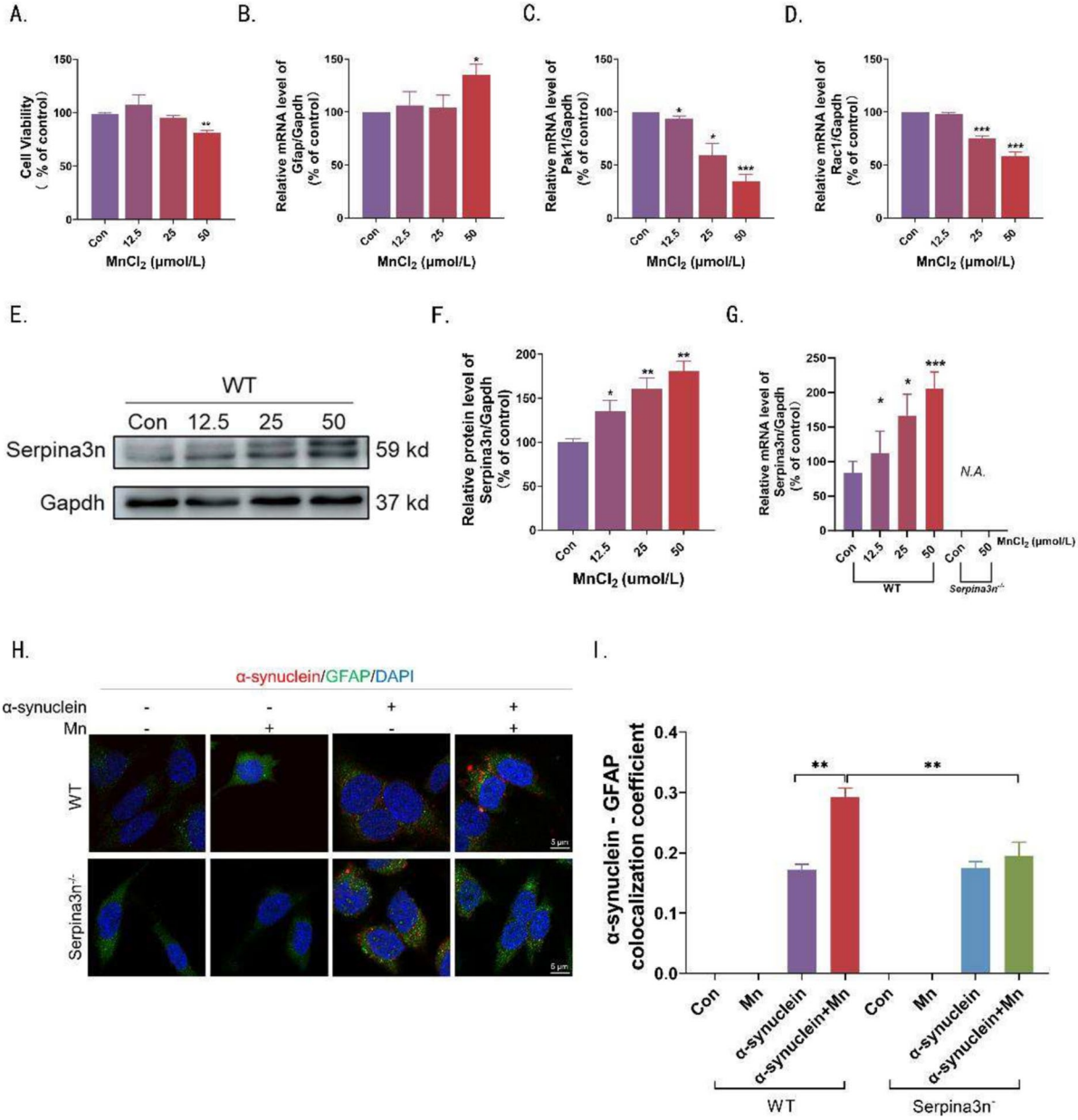

Fig. 3 Mn induced cytotoxicity and disrupted α-Syn clearance in C8-D1A cells. **A**: Dose-dependent change of cell viability measured at 24 h after treatment with different concentrations of $MnCl_2$ (0, 12.5, 25, 50 μmol/L). **B**-**D**: The mRNA levels of *Gfap*, *Pak1* and *Rac1* were determined after different concentrations of Mn treatment at 24 h. **E**–**F**: The protein level and semi-quantitative analysis of Serpina3n after Mn exposure for 24 h. **G**: The mRNA expression of *Serpina3n* in WT and *Serpina3n* KO C8-D1A cells treated with indicated concentrations of Mn for 24 h. **H**-**I**: Immunofluorescence co-localization analysis of intracellular α-Syn (red) with GFAP (green) after Mn exposure (50 μmol/L) in the absence or presence of 0.8 μg/mL α-Syn for 24 h in WT and *Serpina3n* KO C8-D1A cells. Scale bar: 50 μm. The values are presented as means ± SEM. Each experiment was employed at least three times. $*p < 0.05$, $**p < 0.01$, $***p < 0.001$ vs control

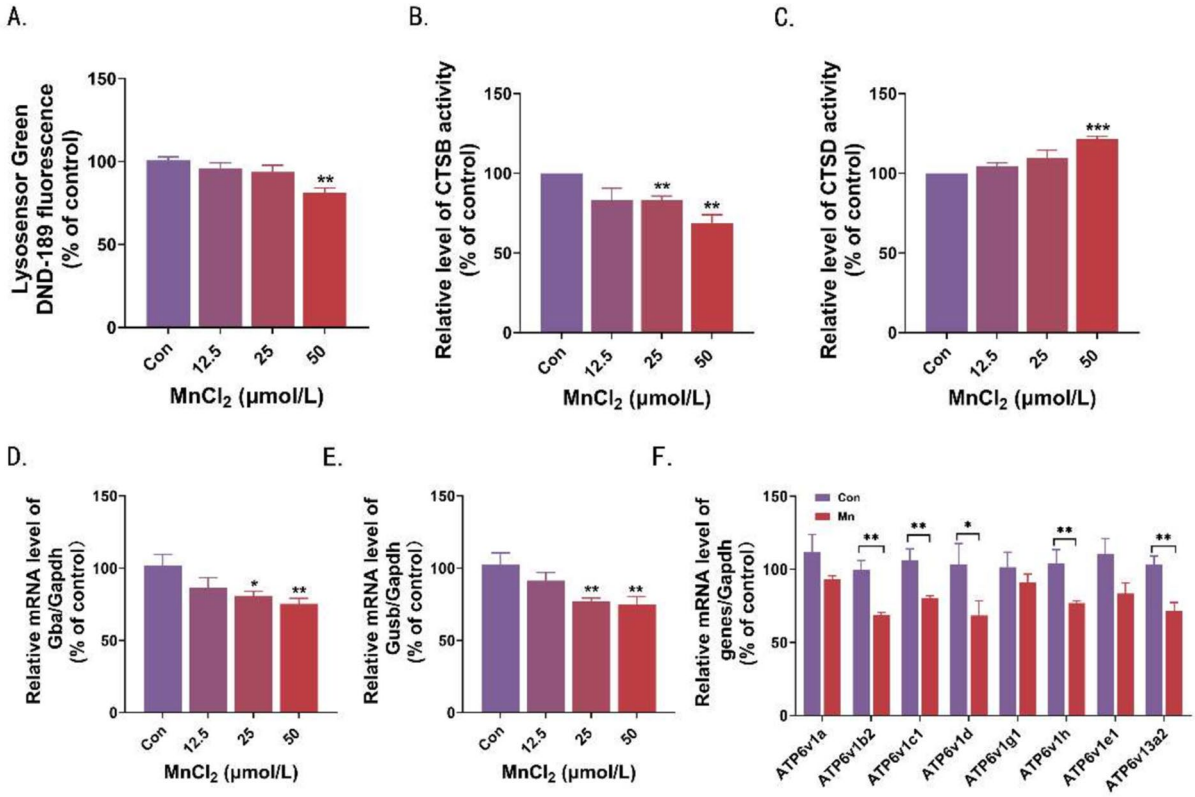

Fig. 4 Mn impaired lysosome function in C8-D1A cells. C8-D1A cells were treated with different concentrations of $MnCl_2$ (0, 12.5, 25, 50 μmol/L). **A**: Lysosomal acidic environment was measured by LysoSensor DND-189 fluorescence intensity. **B**-**C**: CTSB and CTSD activities were detected using corresponding assay kits. **D**-**E**: Changes of mRNA expression of *Gba* and *Gusb*. **F**: The mRNA levels of H^+ transporting ATPase in C8-D1A cells after Mn exposure (50 μmol/L) for 24 h. The values are presented as means ± SEM. Each experiment was employed at least three times. $^*p < 0.05$, $^{**}p < 0.01$, $^{***}p < 0.001$ vs control

treatment. As shown in Fig. 4A, Mn at 50 μmol/L for 24 h induced a significant reduction in H^+ concentration ($P < 0.05$). Meanwhile, the catalytic activity of CTSB in the lysosome was dose-dependently decreased ($P < 0.01$; Fig. 4B), while the CTSD activity was significantly increased after Mn exposure for 24 h ($P < 0.001$ at 50 μmol/L; Fig. 4C). The mRNA expression of genes encoding lysosomal enzymes (*Gba* and *Gusb*) and genes regulating lysosomal acidification homeostasis (V/P-ATPases) were also determined (Colacurcio and Nixon 2016; Fujii et al. 2023). Our data suggested that Mn induced a substantial decrease in the mRNA expression of *Gba*, *Gusb*, *ATP6v1b2*, *ATP6v1c1*, *ATP6v1d*, *ATP6v1h* and *ATP6v13a2* (Fig. 4E-G). These results clearly indicated that Mn induced lysosomal acidification defects in C8-D1A cells.

Serpina3n KO alleviated Mn-induced reduction of Lamp1 and Lamp2 in astrocytes and mouse midbrain

Lysosome-associated membrane proteins (LAMP-1 and LAMP-2) are essential for keeping a highly acidic PH in lysosome and are widely recognized as lysosomal markers (Zhang et al. 2023). Having confirmed that Serpina3n plays an important role in Mn-induced neurotoxicity, we then examined the protein levels of Lamp1 and Lamp2 in *Serpina3n* KO C8-D1A cell after Mn exposure. We found that Serpina3n KO apparently attenuated the reduced protein expression of Lamp1 and Lamp2 caused by Mn (Fig. 5A-C). In parallel, Mn led to a significant reduction of Lamp1 and Lamp2 in the mouse midbrain, while the reduction of Lamp2 was also attenuated by Serpina3n deletion in mice (Fig. 5D-F). To dissect the

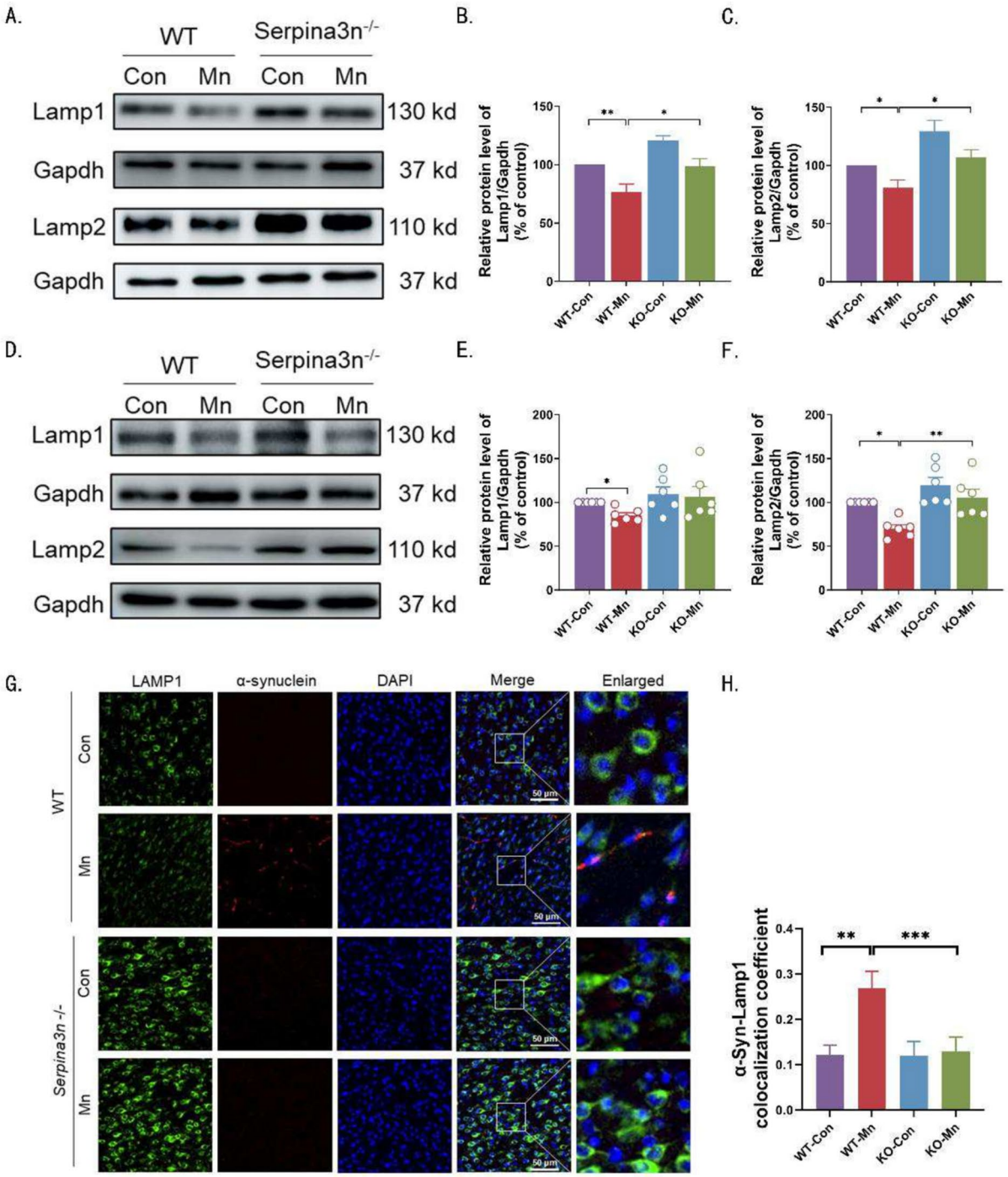

Fig. 5 *Serpina3n* KO alleviated Mn-induced reduction of Lamp1 and Lamp2 in astrocytes and mouse midbrain. **A**: The protein level of Lamp1 ($n=5$) and Lamp2 ($n=4$) in WT and *Serpina3n* KO C8-D1A cells treated with 50 μM $MnCl_2$ for 24 h. **B**-**C**: Semi-quantitative analysis. **D**: The protein level of Lamp1 and Lamp2 in mice midbrain after Mn exposure for 6 weeks. **E**–**F**: Semi-quantitative analysis ($n=6$). G: Immunofluorescent co-localization analysis of Lamp1 (green) with α-Syn (red) and semi-quantitative analysis in the striatum of mice. Scale bar: 50 μm. H: 8 non-overlapping areas of the midbrain of 4 mice (sex ratio 1:1) were assigned for semi-quantitative analysis. The values are presented as means ± SEM. * $p<0.05$, ** $p<0.01$

correlation between lysosomal dysfunction and α-Syn aggregation *in vivo*, immunofluorescence co-localization analysis of α-Syn with Lamp1 was performed in mouse midbrain. It was shown that *Serpina3n* KO apparently reversed Mn-induced Lamp1 immunofluorescence decrease and α-Syn immunofluorescence increase (Fig. 5G-H). Therefore, our results showed that *Serpina3n* KO alleviated the Mn-induced reduction of Lamp1 and Lamp2 in astrocytes and mouse midbrain.

TFEB-v/p ATPases signaling was involved in the Serpina3n-mediated antagonism for Mn-induced lysosome dysfunction in C8-D1A cells

Lysosomes are multifunctional signaling hubs that integrate environmental cues and are tightly regulated by several transcription factors, in particular TFEB (Hesketh et al. 2018). Recent literature reported that TFEB-vacuolar ATPase signaling is essential for lysosomal acidification (Wang et al. 2024). To further dissect how Mn exposure disrupts lysosomal function via Serpina3n, the TFEB nuclear translocation was examined. Our data showed that *Serpina3n* KO abrogated Mn-induced nuclear TFEB loss in C8-D1A cells (Fig. 6A-B). In addition, *Serpina3n* KO also ameliorated the Mn-induced downregulation of the mRNA expression of TFEB-targeted genes *GNS*, *TPP1*, *Sgsh*, *Uvrag* and *Gabarap* (Fig. 6C) in C8-D1A cells, which are responsible for coordinating lysosomal biogenesis (Settembre et al. 2011; Zhang et al. 2020a). We then determined the expression of genes encoding V/P-ATPases, which are involved in regulating the acidic environment of the lysosomes. Mn induced reduction of *ATP13A2*, *ATP6v1b2*, *ATP6v1c1*, *ATP6v1d* and *ATP6v1h* mRNA levels was significantly mitigated by Serpina3n deletion in C8-D1A cells (Fig. 6D). Furthermore, Serpina3n deletion reversed the Mn-induced suppression of LysoSensor Green DND-189 fluorescence intensity in C8-D1A cells (Fig. 6E). We then determined the effects of Serpina3n KO on cysteine proteinases. Serpina3n KO attenuated the Mn-induced inhibition of CTSB activity, but had no effect on the Mn-induced increase in CTSD activity (Fig. 6F-G). These data indicated that TFEB-v/p ATPases signaling was involved in the Serpina3n-mediated counteraction against Mn-induced disruption of lysosomal acidic environment in C8-D1A cells.

Collectively, our study demonstrated that Serpina3n deletion attenuates Mn-induced neurotoxicity and alleviates parkinsonism-like symptoms by protecting the astrocytic capacity of α-Syn clearance and preserving lysosomal function mediated by the TFEB-v/p ATPases signaling pathway (Fig. 7).

Discussion

Our present investigation is the first to illuminate that *Serpina3n* KO alleviates Mn-induced parkinsonism-like symptoms by maintaining the lysosomal acidic environment via TFEB-v/p-ATPase signaling to enhance α-Syn clearance in astrocytes. Detrimental effects of Serpina3n in Mn neurotoxicity as evidenced by the facts:

(i) Serpina3n deletion attenuates Mn induced locomotor abnormalities and midbrain DA neuronal loss in mice.
(ii) *Serpina3n* KO ameliorates Mn-induced astrocytic α-Syn clearance defects both *in vivo* and *in vitro*.
(iii) Serpina3n KO preserves lysosomal function in astrocytes, which is attributed to the TFEB-v/p-ATPases signaling pathway.

These results highlight the central role of Serpina3n in Mn neurotoxicity associated with parkinsonism.

Mn is an essential dietary mineral and a key component bound to several enzymes in the brain. The tolerable upper intake level of Mn set by the EFSA and the US IOM is 11 mg/day for adults. Occupational welding studies indicated that the respirable Mn at 100–140 μg/m^3 would result in brain deposition of < 1.2 μg/g Mn (Bailey et al. 2018). There is a debate as to whether excessive Mn exposure leads to damage to the nigrostriatal dopaminergic system identical to PD, or whether it causes a pathology distinct from PD, known as manganism (Racette et al. 2012). Because studies in humans and non-human primates have reported that parkinsonism-like manifestations induced by excessive Mn deposition are not attributed to dopaminergic dysfunction or dopamine terminal loss in the striatum (Olanow 2004; Pal et al. 1999). In recent years, this argument has been solved based on a plenty of epidemiological and experimental-based studies

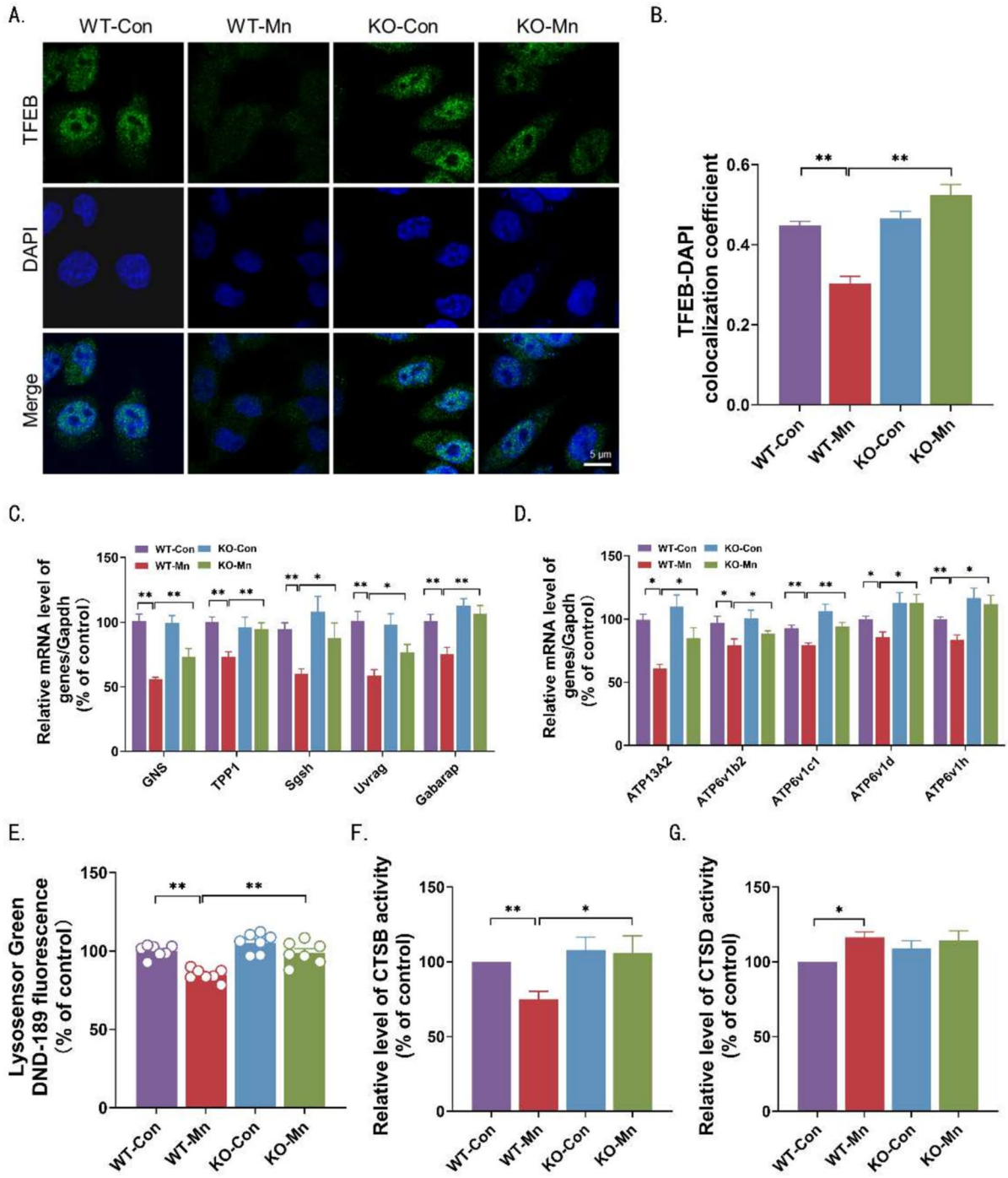

Fig. 6 TFEB-v/p-ATPases signaling was involved in the Serpina3n-mediated counteraction against Mn-induced lysosome dysfunction in C8-D1A cells. Wild type and *Serpina3n* KO C8-D1A cells were treated with 50 μM $MnCl_2$ for 24 h. **A**-**B**: Immunofluorescence analysis of TFEB staining and its semi-quantification. Scale bar: 5 μm. **C**: Changes in mRNA expressions of TFEB target genes. **D**: Changes in mRNA expressions of v/p-ATPases genes. **E**: LysoSensor DND-189 fluorescence intensity. **F**-**G**: CTSB (**F**) and CTSD (**G**) activities. All experiments were repeated at least 3 times. The values are presented as means ± SEM. * $p < 0.05$, ** $p < 0.01$

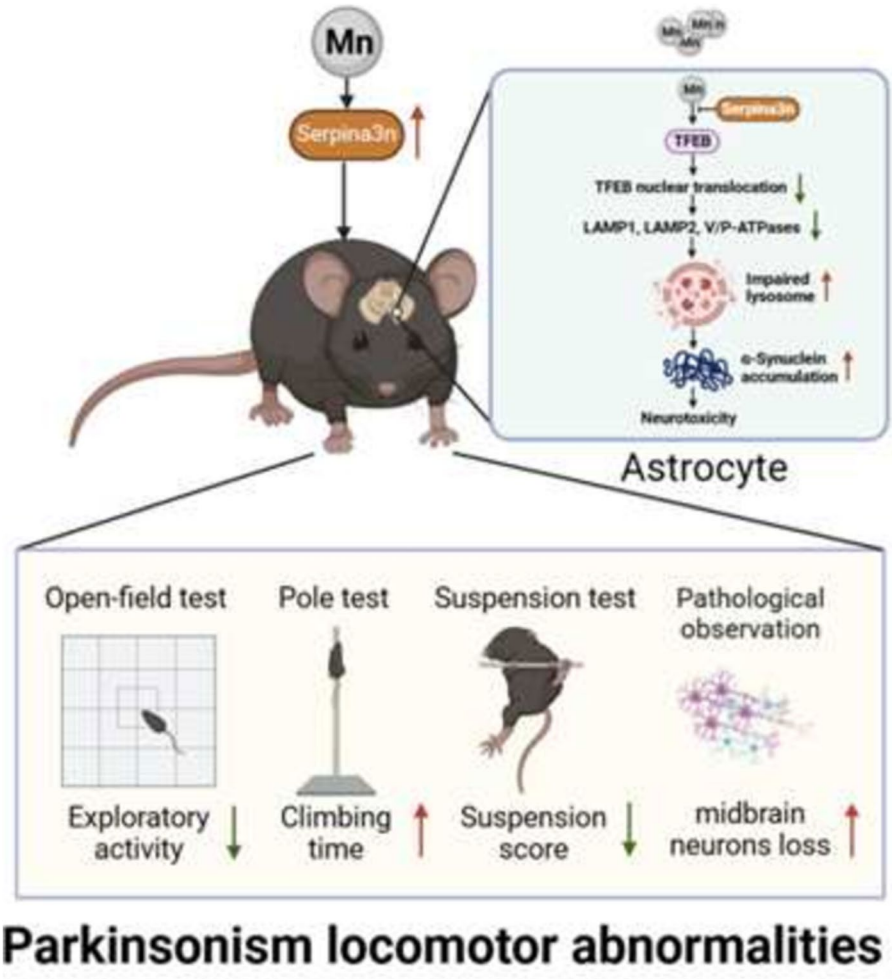

Fig. 7 Graphical abstract. A detrimental role of Serpina3n in Mn-induced Parkinsonism-like symptoms. *Serpina3n* deletion attenuated Mn-induced neurotoxicity and alleviated Parkinsonism-like symptoms by protecting the astrocytic capacity of α-Syn clearance and preserving lysosomal function mediated by TFEB-v/p-ATPases signaling pathway

(Andruska and Racette 2015; Budinger et al. 2021). It was reported that intraperitoneal injections of 25–100 mg/kg/d $MnCl_2{\cdot}4H_2O$ for 1–8 weeks have been widely used to assess neurotoxicity in mice (Ghaisas et al. 2021; Song et al. 2016; Taylor et al. 2020). For example, mice exposed to 50 mg/kg $MnCl_2{\cdot}4H_2O$ (i.p.) for 2 weeks exhibited impaired motor function and DA neurodegeneration (Deng et al. 2015; Qi et al. 2020a). While mice treated with 100 mg/kg $MnCl_2{\cdot}4H_2O$ (i.p.) for 8 weeks displayed significant motor defects and decreased midbrain DA content (Liu et al. 2006). In our study, mice were treated with 32.5 mg/kg $MnCl_2$ (i.p.) for 6 weeks and a phenotype related to the clinical manifestation of PD and typical loss of TH-positive neurons in the SNpc was observed, which is consistent with the above study (Deng et al. 2015). This study helps to establish a causal link between excessive exposure to essential trace elements and the development of PD-like symptoms.

Despite the genetic, environmental, aging and other factors, α-Syn pathology is widely accepted as a crucial mechanism underlying the etiology of PD (Collaborators 2018; Poewe et al. 2017). Of note, astrocytes have attracted much attention for their ability to clear deleterious α-Syn aggregates. It has been reported that astrocytes can ingest α-Syn released from injured neurons and elicit inflammation (Wang et al. 2024). Subsequently, the ingested α-Syn is eliminated by the ubiquitin–proteasome, lysosomal machinery, tunneling nanotubes, etc. (Lopes da Fonseca et al. 2015; Scheiblich et al. 2021). Our present study found that Mn induced reduction of lysosomal CTSB activity, downregulation of v/p-ATPase expression and inhibition of lysosomal acidification, leading to lysosomal dysfunction. Consistently, Zhang

et al. also reported that Mn decreased the nuclear localization of TFEB and induced lysosomal dysfunction (Zhang et al. 2020a). However, a significant increase in CTSD activity was also observed in the study, which may be a compensatory response to the reduction in CTSB activity. Nevertheless, previously described molecular mechanisms of Mn neurotoxicity are mainly attributed to oxidative stress, neuroinflammation, mitochondrial dysfunction and excitotoxicity (Nyarko-Danquah et al. 2020). Our study is the first to focus on the role of lysosomal impairment in α-Syn pathology and parkinsonism development.

The lysosome has traditionally been considered as a static organelle responsible for degrading the cellular protein aggregates, macromolecules, and other organelles. Recent discoveries underscore the significance of impaired lysosomal homeostasis in contributing to the progression of several neurodegenerative diseases, including PD, AD and frontotemporal degeneration (Udayar et al. 2022). TFEB is a well-known master controller of the lysosomal pathway, responding to lysosomal pH and content by shuttling between the cytoplasm and nucleus, and eliciting its function via engaging with the expression of the coordinated lysosomal genes within the nucleus (Franco-Juarez et al. 2022; Martini-Stoica et al. 2016). Our study indicated that Mn induced nuclear TFEB loss in astrocytes and inhibited the expression of lysosomal acidic environment related v/p-ATPases. TFEB is a master transcriptional regulator of lysosomal biogenesis (Li et al. 2022). While the lysosomal behaviour is influenced by its intracellular pH, which is coordinated by proton pumps, the vacuolar ATPase (v-ATPase) and the p-ATPase (Abu-Remaileh et al. 2017; Jewell et al. 2013). It has been suggested that lysosomal deacidification and dysfunction are common factors in genetic, sporadic and toxin-induced parkinsonism (Colacurcio and Nixon 2016). Of interest, recent literature has demonstrated the physiological significance of TFEB-v-ATPase signaling in microglia via preserving lysosomal homeostasis and modulating immune response (Wang et al. 2024). The p-ATPase ATP13A2 is a lysosomal polyamine exporter whose mutation results in lysosomal dysfunction and is associated with PD (Lopes da Fonseca et al. 2015). The v-ATPase, on the other hand, is a multisubunit complex that performs ATP hydrolysis and affects the lysosomal phenotype (Abu-Remaileh et al. 2017). However, how Mn interferes with TFEB-v/p-ATPase signaling has not been thoroughly investigated in our study. There is still a lack of knowledge about the connections between the genetic alterations of different v/p-ATPase subunits and the aetiology of PD.

Recent studies have considered Serpina3n as a potential therapeutic approach based on its reported implications in CNS insults (Zhu et al. 2024). Clinically, Serpina3n dysregulation is observed in brain cells, plasma and cerebrospinal fluid during various neurological conditions (Zhu et al. 2024). In addition, Serpina3n is considered as a reliable biomarker of astrocytic activation in the unconditioned CNS (Clarke et al. 2018; Kenigsbuch et al. 2022). The therapeutic role of Serpina3n in reducing neuropathic pain by inhibiting leukocyte elastase has also been discovered (Vicuna et al. 2015). Single-nucleus transcriptomics of glial cells from mouse models of AD revealed upregulation of Serpina3n, suggesting its participation in the pathogenesis of AD (Zhou et al. 2020). In our study, we found that *Serpina3n* KO attenuated Mn-induced motor defects, DA neuronal loss and α-Syn accumulation in mice. Meanwhile, Mn-induced lysosomal dysfunction via TFEB-v/p-ATPase signaling was also mitigated by Serpina3n deletion, which protected against the accumulation of α-Syn aggregates. These novel findings not only demonstrated the detrimental role of Serpina3n in Mn neurotoxicity, but also captured the biological functions of Serpina3n in regulating astrocytic α-Syn metabolism and lysosomal homeostasis, emphasizing the possibility of Serpina3n as a pharmacological target for clinical intervention of parkinsonism.

Our study has several limitations. First, the interval between the pole-climbing and suspension tests is not more than 48 h to ensure that the mice have sufficient time to rest, which could affect their performance due to fatigue, thus reducing the reliability and validity of the neurobehavioural tests. As previously reported, aSyn undergoes a phosphorylation modification such as Ser129 to adopt a toxic β-sheet conformation capable of aggregation (Ye et al. 2023). The second limitation is that the phosphorylated Ser129 α-Syn and toxic α-Syn were not further dissected to further confirm the link between astrocyte α-Syn clearance and the role of Serpina3n in respect of parkinsonism-like motor dysfunction. Thirdly, the in situ lysosomal function and

consequent changes in autophagy flux have not been fully investigated. Autophagy is a functional pathway delivering intracytoplasmic contents to the lysosome and is triggered as an important pathogenic process in the neurodegenerative disease, particularly parkinsonism (Menzies et al. 2017). Whether autophagy is involved in Serpina3n-mediated Mn-induced neurotoxicity requires further investigation in the future. Finally, the study did not investigate Mn levels and its metabolism, which is a potential mechanism of Serpina3n-mediated antagonization of Mn-induced neurotoxicity.

Conclusion

In conclusion, the present study unravels an unappreciated role of Serpina3n as a detrimental factor in both Mn neurotoxicity and parkinsonism pathogenesis. Serpina3n deletion attenuates Mn neurotoxicity and alleviates parkinsonism-like symptoms by protecting the astrocytic capacity of α-Syn clearance and preserving lysosomal functions via the TFEB-v/p-ATPase signaling pathway. These results provide new insights into the causal link between Mn neurotoxicity and the development of parkinsonism and identify the Serpina3n as a potential target for antagonizing Mn neurotoxicity in parkinsonism.

Acknowledgements This study was supported by the National Natural Science Foundation of China (No. 82373539, 82404219), Postdoctoral Fellowship Program of CPSF (No. GZC20233316) and Foundation of Chongqing Key Laboratory of Prevention and Treatment for Occupational Diseases and Poisoning (Grant No. 2025ZYBKF01).

Author contributions H.H.H: Data Curation, Validation, Writing-Original Draft, Visualization, Funding acquisition. S.C.L, T.Y, J.X.L, K.L, Y.D.X, Y.X, L.L.Y: Project administration. T. L: Visualization. Y.Q.L: Data Curation, Writing-Review & Editing. W.Y: Conceptualization, Supervision. Z.Z: Conceptualization, Supervision, Funding acquisition.

Data availability No datasets were generated or analysed during the current study.

Declarations

Ethical approval The animal studies were approved by Zhejiang University Ethnics Committee of Animal Care and Research (No: RN, 2019-771-1).

Competing interests The authors declare no competing interests.

References

Abu-Remaileh M, Wyant GA, Kim C, Laqtom NN, Abbasi M, Chan SH, Freinkman E, Sabatini DM. Lysosomal metabolomics reveals V-ATPase- and mTOR-dependent regulation of amino acid efflux from lysosomes. Science. 2017;358:807–13. https://doi.org/10.1126/science.aan6298.

Andruska KM, Racette AB. Neuromythology of manganism. Curr Epidemiol Rep. 2015;2:143–8. https://doi.org/10.1007/s40471-015-0040-x.

Aslam MS, Yuan L. Serpina3n: Potential drug and challenges, mini review. J Drug Target. 2020;28:368–78. https://doi.org/10.1080/1061186X.2019.1693576.

Bailey LA, Kerper LE, Goodman JE. Derivation of an occupational exposure level for manganese in welding fumes. Neurotoxicology. 2018;64:166–76. https://doi.org/10.1016/j.neuro.2017.06.009.

Booth HDE, Hirst WD, Wade-Martins R. The role of astrocyte dysfunction in parkinson's disease pathogenesis. Trends Neurosci. 2017;40:358–70. https://doi.org/10.1016/j.tins.2017.04.001.

Budinger D, Barral S, Soo AKS, Kurian MA. The role of manganese dysregulation in neurological disease: emerging evidence. Lancet Neurol. 2021;20:956–68. https://doi.org/10.1016/S1474-4422(21)00238-6.

Calne DB, Chu NS, Huang CC, Lu CS, Olanow W. Manganism and idiopathic parkinsonism: similarities and differences. Neurology. 1994;44:1583–6. https://doi.org/10.1212/wnl.44.9.1583.

Chen C, Ma Q, Chen X, Zhong M, Deng P, Zhu G, Zhang Y, Zhang L, Yang Z, Zhang K, Guo L, Wang L, Yu Z, Zhou Z. Thyroid hormone-Otx2 signaling is required for embryonic ventral midbrain neural stem cells differentiated into dopamine neurons. Stem Cells Dev. 2015;24:1751–65. https://doi.org/10.1089/scd.2014.0489.

Clarke LE, Liddelow SA, Chakraborty C, Munch AE, Heiman M, Barres BA. Normal aging induces A1-like astrocyte reactivity. Proc Natl Acad Sci U S A. 2018;115:E1896–905. https://doi.org/10.1073/pnas.1800165115.

Colacurcio DJ, Nixon RA. Disorders of lysosomal acidification-The emerging role of v-ATPase in aging and neurodegenerative disease. Ageing Res Rev. 2016;32:75–88. https://doi.org/10.1016/j.arr.2016.05.004.

Collaborators GBDPsD. Global, regional, and national burden of Parkinson's disease, 1990–2016: a systematic analysis for the global burden of disease study 2016. Lancet Neurol. 2018;17:939–53. https://doi.org/10.1016/S1474-4422(18)30295-3

Crowe AR, Yue W. Semi-quantitative determination of protein expression using immunohistochemistry staining and analysis: An Integrated Protocol. Bio Protoc. 2019;9. https://doi.org/10.21769/BioProtoc.3465

Deng Y, Jiao C, Mi C, Xu B, Li Y, Wang F, Liu W, Xu Z. Melatonin inhibits manganese-induced motor dysfunction and neuronal loss in mice: involvement of oxidative stress and dopaminergic neurodegeneration. Mol Neurobiol. 2015;51:68–88. https://doi.org/10.1007/s12035-014-8789-3.

Dunn KW, Kamocka MM, McDonald JH. A practical guide to evaluating colocalization in biological microscopy. Am J Physiol Cell Physiol. 2011;300:C723–42. https://doi.org/10.1152/ajpcell.00462.2010.

Fan X, Luo G, Yang D, Ming M, Liu H, Pu P, Le W. Critical role of lysosome and its associated protein cathepsin D in manganese-induced toxicity in cultured midbrain astrocyte. Neurochem Int. 2010;56:291–300. https://doi.org/10.1016/j.neuint.2009.11.001.

Fellner L, Irschick R, Schanda K, Reindl M, Klimaschewski L, Poewe W, Wenning GK, Stefanova N. Toll-like receptor 4 is required for alpha-synuclein dependent activation of microglia and astroglia. Glia. 2013;61:349–60. https://doi.org/10.1002/glia.22437.

Franco-Juarez B, Coronel-Cruz C, Hernandez-Ochoa B, Gomez-Manzo S, Cardenas-Rodriguez N, Arreguin-Espinosa R, Bandala C, Canseco-Avila LM, Ortega-Cuellar D. TFEB; Beyond its role as an autophagy and lysosomes regulator. Cells. 2022;11. https://doi.org/10.3390/cells11193153

Fujii T, Nagamori S, Wiriyasermkul P, Zheng S, Yago A, Shimizu T, Tabuchi Y, Okumura T, Fujii T, Takeshima H, Sakai H. Parkinson's disease-associated ATP13A2/PARK9 functions as a lysosomal H(+), K(+)-ATPase. Nat Commun. 2023;14:2174. https://doi.org/10.1038/s41467-023-37815-z.

Ghaisas S, Harischandra DS, Palanisamy B, Proctor A, Jin H, Dutta S, Sarkar S, Langley M, Zenitsky G, Anantharam V, Kanthasamy A, Phillips GJ, Kanthasamy A. Chronic manganese exposure and the enteric nervous system: An *in vitro* and mouse *in vivo* study. Environ Health Perspect. 2021;129:87005. https://doi.org/10.1289/EHP7877.

Gillispie EC, Austin RE, Rivera NA, Bolich R, Duckworth OW, Bradley P, Amoozegar A, Hesterberg D, Polizzotto ML. Soil weathering as an engine for manganese contamination of well water. Environ Sci Technol. 2016;50:9963–71. https://doi.org/10.1021/acs.est.6b01686.

Haile Y, Carmine-Simmen K, Olechowski C, Kerr B, Bleackley RC, Giuliani F. Granzyme B-inhibitor serpina3n induces neuroprotection *in vitro* and *in vivo*. J Neuroinflammation. 2015;12:157. https://doi.org/10.1186/s12974-015-0376-7.

Harischandra DS, Rokad D, Neal ML, Ghaisas S, Manne S, Sarkar S, Panicker N, Zenitsky G, Jin H, Lewis M, Huang X, Anantharam V, Kanthasamy A, Kanthasamy AG. Manganese promotes the aggregation and prion-like cell-to-cell exosomal transmission of alpha-synuclein. Sci Signal. 2019;12. https://doi.org/10.1126/scisignal.aau4543

Hesketh GG, Wartosch L, Davis LJ, Bright NA, Luzio JP. The Lysosome and Intracellular Signalling. Prog Mol Subcell Biol. 2018;57:151–80. https://doi.org/10.1007/978-3-319-96704-2_6.

Jewell JL, Russell RC, Guan KL. Amino acid signalling upstream of mTOR. Nat Rev Mol Cell Biol. 2013;14:133–9. https://doi.org/10.1038/nrm3522.

Jiang Y, Lin Y, Tetlow AM, Pan R, Ji C, Kong XP, Congdon EE, Sigurdsson EM. Single-Domain antibody-based protein degrader for synucleinopathies. bioRxiv. 2024. https://doi.org/10.1101/2024.03.11.584473

Jiang YM, Mo XA, Du FQ, Fu X, Zhu XY, Gao HY, Xie JL, Liao FL, Pira E, Zheng W. Effective treatment of manganese-induced occupational Parkinsonism with p-aminosalicylic acid: a case of 17-year follow-up study. J Occup Environ Med. 2006;48:644–9. https://doi.org/10.1097/01.jom.0000204114.01893.3e.

Karri V, Schuhmacher M, Kumar V. Heavy metals (Pb, Cd, As and MeHg) as risk factors for cognitive dysfunction: A general review of metal mixture mechanism in brain. Environ Toxicol Pharmacol. 2016;48:203–13. https://doi.org/10.1016/j.etap.2016.09.016.

Kenigsbuch M, Bost P, Halevi S, Chang Y, Chen S, Ma Q, Hajbi R, Schwikowski B, Bodenmiller B, Fu H, Schwartz M, Amit I. A shared disease-associated oligodendrocyte signature among multiple CNS pathologies. Nat Neurosci. 2022;25:876–86. https://doi.org/10.1038/s41593-022-01104-7.

Kim S, Kwon SH, Kam TI, Panicker N, Karuppagounder SS, Lee S, et al. Transneuronal propagation of pathologic α-synuclein from the gut to the brain models Parkinson's disease. Neuron. 2019;103(4):627–41. https://doi.org/10.1016/j.neuron.2019.05.035.

Lee HJ, Suk JE, Bae EJ, Lee SJ. Clearance and deposition of extracellular alpha-synuclein aggregates in microglia. Biochem Biophys Res Commun. 2008;372:423–8. https://doi.org/10.1016/j.bbrc.2008.05.045.

Leonard JD, Gilmore DC, Dileepan T, Nawrocka WI, Chao JL, Schoenbach MH, Jenkins MK, Adams EJ, Savage PA. Identification of natural regulatory T cell epitopes reveals convergence on a dominant autoantigen. Immunity. 2017;47:107–17. https://doi.org/10.1016/j.immuni.2017.06.015.

Li M, Pi H, Yang Z, Reiter RJ, Xu S, Chen X, Chen C, Zhang L, Yang M, Li Y, Guo P, Li G, Tu M, Tian L, Xie J, He M, Lu Y, Zhong M, Zhang Y, Yu Z, Zhou Z. Melatonin antagonizes cadmium-induced neurotoxicity by activating the transcription factor EB-dependent autophagy-lysosome machinery in mouse neuroblastoma cells. J Pineal Res. 2016;61:353–69. https://doi.org/10.1111/jpi.12353.

Li T, Yin L, Kang X, Xue W, Wang N, Zhang J, Yuan P, Lin L, Li Y. TFEB acetylation promotes lysosome biogenesis and ameliorates Alzheimer's disease-relevant phenotypes

in mice. J Biol Chem. 2022;298. https://doi.org/10.1016/j.jbc.2022.102649.

Lindstrom V, Gustafsson G, Sanders LH, Howlett EH, Sigvardson J, Kasrayan A, Ingelsson M, Bergstrom J, Erlandsson A. Extensive uptake of alpha-synuclein oligomers in astrocytes results in sustained intracellular deposits and mitochondrial damage. Mol Cell Neurosci. 2017;82:143–56. https://doi.org/10.1016/j.mcn.2017.04.009.

Liu X, Sullivan KA, Madl JE, Legare M, Tjalkens RB. Manganese-induced neurotoxicity: the role of astroglial-derived nitric oxide in striatal interneuron degeneration. Toxicol Sci. 2006;91:521–31. https://doi.org/10.1093/toxsci/kfj150.

Lopes da Fonseca T, Villar-Pique A, Outeiro TF. The Interplay between Alpha-Synuclein Clearance and Spreading. Biomolecules. 2015;5:435–71. https://doi.org/10.3390/biom5020435

Lucchini RG, Aschner M, Landrigan PJ, Cranmer JM. Neurotoxicity of manganese: Indications for future research and public health intervention from the Manganese 2016 conference. Neurotoxicology. 2018;64:1–4. https://doi.org/10.1016/j.neuro.2018.01.002.

Ma L, Shen X, Gao Y, Wu Q, Ji M, Luo C, Zhang M, Wang T, Chen X, Tao L. Blocking B7–1/CD28 pathway diminished long-range brain damage by regulating the immune and inflammatory responses in a mouse model of intracerebral hemorrhage. Neurochem Res. 2016;41:1673–83. https://doi.org/10.1007/s11064-016-1883-3.

Ma Z, Liu K, Li XR, Wang C, Liu C, Yan DY, Deng Y, Liu W, Xu B. Alpha-synuclein is involved in manganese-induced spatial memory and synaptic plasticity impairments via TrkB/Akt/Fyn-mediated phosphorylation of NMDA receptors. Cell Death Dis. 2020;11:834. https://doi.org/10.1038/s41419-020-03051-2.

Martini-Stoica H, Xu Y, Ballabio A, Zheng H. The autophagy-lysosomal pathway in neurodegeneration: A TFEB perspective. Trends Neurosci. 2016;39:221–34. https://doi.org/10.1016/j.tins.2016.02.002.

Masini D, Kiehn O. Targeted activation of midbrain neurons restores locomotor function in mouse models of parkinsonism. Nat Commun. 2022;13(1):504. https://doi.org/10.1038/s41467-022-28075-4.

Menezes-Filho JA, Paes CR, Pontes AM, Moreira JC, Sarcinelli PN, Mergler D. High levels of hair manganese in children living in the vicinity of a ferro-manganese alloy production plant. Neurotoxicology. 2009;30:1207–13. https://doi.org/10.1016/j.neuro.2009.04.005.

Menzies FM, Fleming A, Caricasole A, Bento CF, Andrews SP, Ashkenazi A, Fullgrabe J, Jackson A, Jimenez Sanchez M, Karabiyik C, Licitra F, Lopez Ramirez A, Pavel M, Puri C, Renna M, Ricketts T, Schlotawa L, Vicinanza M, Won H, Zhu Y, Skidmore J, Rubinsztein DC. Autophagy and neurodegeneration: Pathogenic mechanisms and therapeutic opportunities. Neuron. 2017;93:1015–34. https://doi.org/10.1016/j.neuron.2017.01.022.

Moors T, Paciotti S, Chiasserini D, Calabresi P, Parnetti L, Beccari T, van de Berg WD. Lysosomal dysfunction and alpha-synuclein aggregation in parkinson's disease: Diagnostic links. Mov Disord. 2016;31:791–801. https://doi.org/10.1002/mds.26562.

Mor DE, Daniels MJ, Ischiropoulos H. The usual suspects, dopamine and alpha-synuclein, conspire to cause neurodegeneration. Mov Disord. 2019;34:167–79. https://doi.org/10.1002/mds.27607.

Morello M, Canini A, Mattioli P, Sorge RP, Alimonti A, Bocca B, Forte G, Martorana A, Bernardi G, Sancesario G. Sub-cellular localization of manganese in the basal ganglia of normal and manganese-treated rats An electron spectroscopy imaging and electron energy-loss spectroscopy study. Neurotoxicology. 2008;29:60–72. https://doi.org/10.1016/j.neuro.2007.09.001.

Nyarko-Danquah I, Pajarillo E, Digman A, Soliman KFA, Aschner M, Lee E. Manganese Accumulation in the Brain via various transporters and its neurotoxicity mechanisms. molecules. 2020;25. https://doi.org/10.3390/molecules25245880

O'Neal SL, Zheng W. Manganese toxicity upon overexposure: A decade in review. Curr Environ Health Rep. 2015;2:315–28. https://doi.org/10.1007/s40572-015-0056-x.

Olanow CW. Manganese-induced parkinsonism and Parkinson's disease. Ann N Y Acad Sci. 2004;1012:209–23. https://doi.org/10.1196/annals.1306.018.

Ommati MM, Heidari R, Ghanbarinejad V, Aminian A, Abdoli N, Niknahad H. The neuroprotective properties of carnosine in a mouse model of manganism is mediated via mitochondria regulating and antioxidative mechanisms. Nutr Neurosci. 2020;23(9):731–43. https://doi.org/10.1080/1028415X.2018.1552399.

Pal PK, Samii A, Calne DB. Manganese neurotoxicity: a review of clinical features, imaging and pathology. Neurotoxicology. 1999;20:227–38.

Poewe W, Seppi K, Tanner CM, Halliday GM, Brundin P, Volkmann J, Schrag AE, Lang AE. Parkinson Disease Nat Rev Dis Primers. 2017;3:17013. https://doi.org/10.1038/nrdp.2017.13.

Porcellini E, Davis EJ, Chiappelli M, Ianni E, Di Stefano G, Forti P, Ravaglia G, Licastro F. Elevated plasma levels of alpha-1-anti-chymotrypsin in age-related cognitive decline and Alzheimer's disease: a potential therapeutic target. Curr Pharm des. 2008;14:2659–64. https://doi.org/10.2174/138161208786264151.

Qi Z, Yang X, Sang Y, Liu Y, Li J, Xu B, Liu W, He M, Xu Z, Deng Y, Zhu J. Correction to: Fluoxetine and riluzole mitigates manganese-induced disruption of glutamate transporters and excitotoxicity via ephrin-A3/GLAST-GLT-1/glu signaling pathway in striatum of mice. Neurotox Res. 2020;38:1061. https://doi.org/10.1007/s12640-020-00281-2.

Qi Z, Yang X, Sang Y, Liu Y, Li J, Xu B, Liu W, He M, Xu Z, Deng Y, Zhu J. Fluoxetine and riluzole mitigates manganese-induced disruption of glutamate transporters and excitotoxicity via Ephrin-A3/GLAST-GLT-1/glu signaling pathway in striatum of mice. Neurotox Res. 2020;38:508–23. https://doi.org/10.1007/s12640-020-00209-w.

Racette BA, Aschner M, Guilarte TR, Dydak U, Criswell SR, Zheng W. Pathophysiology of manganese-associated neurotoxicity. Neurotoxicology. 2012;33:881–6. https://doi.org/10.1016/j.neuro.2011.12.010.

Rannikko EH, Weber SS, Kahle PJ. Exogenous alpha-synuclein induces toll-like receptor 4 dependent inflammatory responses in astrocytes. BMC Neurosci. 2015;16:57. https://doi.org/10.1186/s12868-015-0192-0.

Scheiblich H, Dansokho C, Mercan D, Schmidt SV, Bousset L, Wischhof L, Eikens F, Odainic A, Spitzer J, Griep A, Schwartz S, Bano D, Latz E, Melki R, Heneka MT. Microglia jointly degrade fibrillar alpha-synuclein cargo by distribution through tunneling nanotubes. Cell. 2021;184:5089–106. https://doi.org/10.1016/j.cell.2021.09.007.

Settembre C, Di Malta C, Polito VA, Garcia Arencibia M, Vetrini F, Erdin S, Erdin SU, Huynh T, Medina D, Colella P, Sardiello M, Rubinsztein DC, Ballabio A. TFEB links autophagy to lysosomal biogenesis. Science. 2011;332:1429–33. https://doi.org/10.1126/science.1204592.

Song Q, Deng Y, Yang X, Bai Y, Xu B, Liu W, Zheng W, Wang C, Zhang M, Xu Z. Manganese-disrupted interaction of dopamine D1 and NMDAR in the striatum to injury learning and memory ability of mice. Mol Neurobiol. 2016;53:6745–58. https://doi.org/10.1007/s12035-015-9602-7.

Taylor CA, Tuschl K, Nicolai MM, Bornhorst J, Gubert P, Varao AM, Aschner M, Smith DR, Mukhopadhyay S. Maintaining translational relevance in animal models of manganese neurotoxicity. J Nutr. 2020;150:1360–9. https://doi.org/10.1093/jn/nxaa066.

Tong T, Duan W, Xu Y, Hong H, Xu J, Fu G, Wang X, Yang L, Deng P, Zhang J, He H, Mao G, Lu Y, Lin X, Yu Z, Pi H, Cheng Y, Xu S, Zhou Z. Paraquat exposure induces Parkinsonism by altering lipid profile and evoking neuroinflammation in the midbrain. Environ Int. 2022;169:107512. https://doi.org/10.1016/j.envint.2022.107512.

Udayar V, Chen Y, Sidransky E, Jagasia R. Lysosomal dysfunction in neurodegeneration: emerging concepts and methods. Trends Neurosci. 2022;45:184–99. https://doi.org/10.1016/j.tins.2021.12.004.

Vicuna L, Strochlic DE, Latremoliere A, Bali KK, Simonetti M, Husainie D, Prokosch S, Riva P, Griffin RS, Njoo C, Gehrig S, Mall MA, Arnold B, Devor M, Woolf CJ, Liberles SD, Costigan M, Kuner R. The serine protease inhibitor SerpinA3N attenuates neuropathic pain by inhibiting T cell-derived leukocyte elastase. Nat Med. 2015;21:518–23. https://doi.org/10.1038/nm.3852.

Vollet K, Haynes EN, Dietrich KN. Manganese exposure and cognition across the lifespan: Contemporary review and argument for biphasic dose-response health effects. Curr Environ Health Rep. 2016;3:392–404. https://doi.org/10.1007/s40572-016-0108-x.

Wang B, Martini-Stoica H, Qi C, Lu TC, Wang S, Xiong W, Qi Y, Xu Y, Sardiello M, Li H, Zheng H. TFEB-vacuolar ATPase signaling regulates lysosomal function and microglial activation in tauopathy. Nat Neurosci. 2024;27:48–62. https://doi.org/10.1038/s41593-023-01494-2.

Wang R, Sun H, Ren H, Wang G. alpha-Synuclein aggregation and transmission in Parkinson's disease: a link to mitochondria and lysosome. Sci China Life Sci. 2020;63:1850–9. https://doi.org/10.1007/s11427-020-1756-9.

Xi Y, Liu M, Xu S, Hong H, Chen M, Tian L, Xie J, Deng P, Zhou C, Zhang L, He M, Chen C, Lu Y, Reiter RJ, Yu Z, Pi H, Zhou Z. Inhibition of SERPINA3N-dependent neuroinflammation is essential for melatonin to ameliorate trimethyltin chloride-induced neurotoxicity. J Pineal Res. 2019;67:e12596. https://doi.org/10.1111/jpi.12596.

Ye H, Robak LA, Yu M, Cykowski M, Shulman JM. Genetics and pathogenesis of parkinson's syndrome. Annu Rev Pathol. 2023;18:95–121. https://doi.org/10.1146/annurev-pathmechdis-031521-034145.

Zhang J, Zeng W, Han Y, Lee WR, Liou J, Jiang Y. Lysosomal LAMP proteins regulate lysosomal pH by direct inhibition of the TMEM175 channel. Mol Cell. 2023;83:2524–39. https://doi.org/10.1016/j.molcel.2023.06.004.

Zhang Z, Yan J, Bowman AB, Bryan MR, Singh R, Aschner M. Dysregulation of TFEB contributes to manganese-induced autophagic failure and mitochondrial dysfunction in astrocytes. Autophagy. 2020;16:1506–23. https://doi.org/10.1080/15548627.2019.1688488.

Zhang ZD, Xiong TC, Yao SQ, Wei MC, Chen M, Lin D, Zhong B. RNF115 plays dual roles in innate antiviral responses by catalyzing distinct ubiquitination of MAVS and MITA. Nat Commun. 2020;11:5536. https://doi.org/10.1038/s41467-020-19318-3.

Zhou Y, Song WM, Andhey PS, Swain A, Levy T, Miller KR, Poliani PL, Cominelli M, Grover S, Gilfillan S, Cella M, Ulland TK, Zaitsev K, Miyashita A, Ikeuchi T, Sainouchi M, Kakita A, Bennett DA, Schneider JA, Nichols MR, Beausoleil SA, Ulrich JD, Holtzman DM, Artyomov MN, Colonna M. Human and mouse single-nucleus transcriptomics reveal TREM2-dependent and TREM2-independent cellular responses in Alzheimer's disease. Nat Med. 2020;26:131–42. https://doi.org/10.1038/s41591-019-0695-9.

Zhu M, Lan Z, Park J, Gong S, Wang Y, Guo F. Regulation of CNS pathology by Serpina3n/SERPINA3: The knowns and the puzzles. Neuropathol Appl Neurobiol. 2024;50. https://doi.org/10.1111/nan.12980.